

# Physicochemical characteristic of corn starch nanoparticles obtained by acid hydrolysis method

*Ardhinata Antares*<sup>1</sup>, *Luh Putu Wrasiasi*<sup>2</sup>, *Bambang Admadi Harsojuwono*<sup>2</sup>, *I Wayan Rai Widarta*<sup>3</sup>, *Ni Luh Yulianti*<sup>4</sup>, *Nanang Masruchin*<sup>5</sup>, *Mohamad Nurul Azman Mohammad Taib*<sup>6</sup>, and *I Wayan Arnata*<sup>2\*</sup>

<sup>1</sup>Bachelor of Food Technology Program, Faculty of Technology, Institute of Technology and Health Bali, Bali, Indonesia

<sup>2</sup>Department of Agroindustrial Technology, Faculty of Agricultural Technology, Udayana University, Badung, 80361 Bali, Indonesia

<sup>3</sup>Department of Food Technology, Faculty of Agriculture Technology, Udayana University, Bali, Indonesia

<sup>4</sup>Agricultural Engineering and Biosystems Study Program, Faculty of Agricultural Technology, Udayana University, Badung (80361), Bali, Indonesia

<sup>5</sup>Research Center for Biomass and Bioproduct, National Research and Innovation Agency, Bogor, Indonesia

<sup>6</sup>Institute for Advanced Studies, 50603 Kuala Lumpur, Malaysia

**Abstract.** Native corn starch often lacks the stability and functionality needed for modern formulations. Here, commercial corn starch was acid-hydrolyzed using 2.2 N HCl at 35 °C for 120 h to generate nano-enabled starch (CSNPs) and to probe how selective chain removal alters structure–property relationships. Relative to the untreated control (CS-Control), the hydrolyzed material showed consistently lower amylose (14.78 → 13.61%), swelling power (17.86 → 16.58%), solubility (19.95 → 14.69%), moisture (10.95 → 8.91%), and protein/fat contents. These shifts indicate preferential cleavage of amorphous, less ordered regions, enabling residual chains to repack via stronger hydrogen bonding. FTIR spectra retained the characteristic starch bands without evidence of new chemistry; a slightly more bonded O–H region and a sharper 1150–900 cm<sup>-1</sup> fingerprint supported increased order and reduced amorphous content. Morphology evolved from smooth granules to etched, rounded particles with surface debris (SEM), while TEM revealed tens-to-hundreds-of-nanometers fragments that readily aggregate—consistent with DLS detecting sub-micron to micron-scale populations. Overall, acid hydrolysis yielded a more ordered, nano-enabled starch while highlighting an important practical point: nanoparticles are created, but without an added dispersion step they remain partially aggregated. These insights can guide post-processing (when discrete nanoscale behavior is required).

## 1 Introduction

Biobased polymers underpin sustainable materials, with corn starch as a one of the material due to its abundance, reproducibility, inexpensive, and broad regulatory acceptance in food and packaging industries. Despite these advantages, native corn starch has key limitations: low cold-water solubility, sensitivity to heat and shear, and a tendency to retrograde which reduce its functional stability and processing versatility [1]. These drawbacks hinder its application in high performance products that require thermal stability, mechanical integrity, and functional adaptability.

A promising strategy to overcome these shortcomings involves reducing starch to the nanoscale: nanosized corn starch (≈5–300 nm) increases surface area, can shift crystallinity toward V-type under specific treatments, and disperses more, enhancing hydration, gelatinization, and interfacial interactions [2], [3], [4]. These nanoscale modifications lead to improving the corn starch tensile strength, low water vapor permeability, and enhanced oxygen barrier properties—attributes critical for applications such as biodegradable films and food coatings. Moreover, nanoscale starch systems can be

engineered for encapsulation and controlled release of bioactive compounds, with surface modifications such as acetylation or succinylation enhancing encapsulation efficiency and stability [5]. The incorporation of polyphenols and surfactants to modulate digestibility, increase resistant starch content, and improve nanoparticle stability [6].

Among the various fabrication methods such as ultrasonication, nanoprecipitation, and enzymatic treatment, acid hydrolysis remains a particularly practical and cost-effective approach for producing starch nanoparticles. While enzymatic hydrolysis offers high specificity and eco-friendly processing conditions, it is often limited by high enzyme costs, slower reaction rates, and the need for strict control over pH and temperature to maintain enzyme activity. In contrast, acid hydrolysis remains the preferred industrial route for starch nanoparticle production due to its speed, cost-effectiveness, and ability to generate high-crystallinity particles by rapidly eroding amorphous regions [2], [7]. Although acid treatment generates chemical waste requiring neutralization, it is significantly more efficient at producing the initial 'top-down' degradation needed to isolate nanoscale crystalline platelets. The technique

\*Corresponding email: [arnata@unud.ac.id](mailto:arnata@unud.ac.id)

selectively cleaves glycosidic bonds within the amorphous regions of starch granules, leading to partial degradation followed by molecular rearrangement into nanostructured particles. While acid hydrolysis reduces molecular weight by cleaving glycosidic bonds, it paradoxically leads to reduced amylose and solubility [7], [8]. This occurs because the treatment selectively degrades amorphous regions, leaving behind highly ordered crystalline fragments that undergo molecular rearrangement [9], [10]. This increased structural order and the subsequent formation of dense aggregates significantly restrict water penetration, resulting in lower solubility and swelling power [8], [11], [12]. Hydrolysis temperature, acid concentration, and time shape the final profile; in our case, 2.2 N HCl at moderate temperature for a controlled duration balanced crystallinity, yield, and colloidal stability [9].

Recent investigations have confirmed that acid hydrolysis of starch can refine its morphology, functional properties for advanced applications. For example, nanoparticles derived from acid-modified corn starch exhibit particle sizes around 150–250 nm with negative zeta potentials (–30 to –45 mV), suggesting good colloidal stability [12]. Moreover, combined acid hydrolysis and ultrasonication treatments have been shown to improve particle uniformity and thermal performance while preserving essential crystallinity [8]. Such physicochemical transformations directly can improve its functionality in films, emulsions, and nutraceutical delivery systems.

The preparation of corn starch nanoparticles (CSNPs) using acid hydrolysis, focusing on detailed characterization of their composition, solubility, spectroscopic behaviour, morphology, and colloidal properties. By systematically analyses how hydrolysis parameters affect the physicochemical attributes of CSNPs, this work aims to establish a foundation for optimizing process conditions that yield nanoparticles with desirable stability, dispersibility, and functional performance. The resulting insights can facilitate the application of CSNPs in high-value biobased products such as functional foods, drug delivery systems, and biodegradable films.

## 2 Materials and Methods

The study used commercial corn starch (Maizenaku) bought from a local supermarket. Standard reagents for starch modification and analysis were employed, including HCl (for hydrolysis), NaOH (for neutralization), ethanol, and analytical chemicals. The native starch was first characterized for key physicochemical properties moisture, protein, fat, swelling power, solubility, amylose, and microstructure (SEM, PSA, PDI, and surface tension).

Hydrolyzed (lintnerized) starch was then prepared following Mohsin et al., [9] with modifications: starch was dispersed in 2.2 N HCl at a 1:2 (w/v) ratio and incubated at 35 °C for 120 h in a shaking water bath. After hydrolysis, the slurry was neutralized to pH ~6.0 with 1 M NaOH, washed with deionized water and ethanol, oven dried at 50

°C for 24 h to ~10% moisture, milled, sieved, and stored. The resulting lintnerized starch was evaluated again for composition (moisture, protein, fat, amylose) [13], functional properties like swelling [14], solubility [8], and structure using (FTIR, zeta potential, Polydispersity Index, particle size analysis) [15], morphology SEM [16] and TEM) [15].

## 3 Results and discussion

### 3.1 Composition and solubility

In the figure 1 shows that the acid-hydrolyzed starch (CSNPs) has a slight reduction in amylose, from about  $14.78 \pm 0.40\%$  in CS-Control to  $13.61 \pm 0.29\%$  in CSNPs. This is in line with the accepted view that mineral acids degrade the less ordered, amylose-rich or amorphous segments first, generating shorter chains that no longer respond to the colorimetric/iodine assay as amylose. Short-chain fragments also repack more easily, so the material behaves less retro-gradable and less swellable.

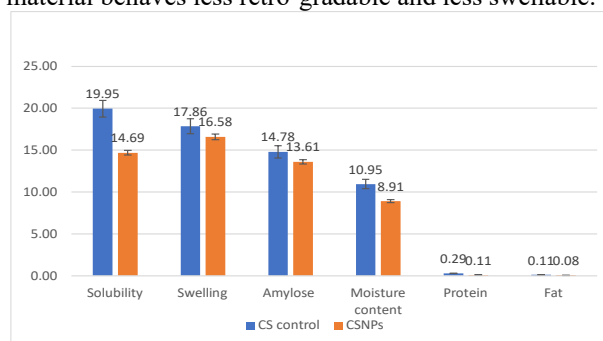


Fig. 1. Composition of CSNPs and CS-Control

Swelling power decreased from  $17.86 \pm 1.30$  to  $16.58 \pm 0.86$ , and water solubility also dropped. This is a common outcome of amorphous-first acid hydrolysis: once the easy to hydrate domains are removed, water has less entry points into the granule and the remaining fractions are more densely hydrogen bonded [17] SEM later confirmed that the granule surface was etched, while FTIR showed a stronger, slightly red-shifted O–H band, both of which support this interpretation. From an application point of view, this means dimensional and thermal stability improve (good for films/coatings and thermal processing), but rapid, high swelling at low temperature becomes less likely.

Moisture content also down, from  $10.95 \pm 0.26\%$  in CS-Control to  $8.91 \pm 0.63\%$  in CSNPs. A more tight and more ordered microstructure can hold less bulk-like water; the water that remains is mainly surface-bound, which is in line with the modest change still showed at  $\sim 1649 \text{ cm}^{-1}$  in FTIR. Lower residual moisture is beneficial for storage stability and for downstream drying. Finally, protein ( $0.29 \rightarrow 0.11\%$ ) and fat ( $0.11 \rightarrow 0.08\%$ ) both decreased, most likely because the hydrolysis–washing sequence stripped loosely bound non-starch components. This cleaner composition is desirable when the material is to be used as food-contact film, coating, or as a carrier for bio actives [10].

### 3.2 Functional groups (FTIR)

The FTIR spectra of CSNPs (Figure 2) confirm that the 2.2 N HCl treatment resulted in structural reorganization rather than chemical derivatization, as all characteristic starch bands were retained without the emergence of new peaks. The primary spectral changes—a slight red-shift and broadening of the O–H stretch (3600–3200  $\text{cm}^{-1}$ ) alongside a stable C–H stretch (2937 $\text{cm}^{-1}$ ) signify stronger intermolecular hydrogen bonding as surviving amylopectin chains re-associate into compact microdomains after the removal of amorphous zones [18]. This intensity redistribution without new peak formation aligns with recent research on starch-cellulose co-processing, which characterizes such patterns as physical embedding and molecular rearrangement rather than the synthesis of new chemical bonds [19], [20]

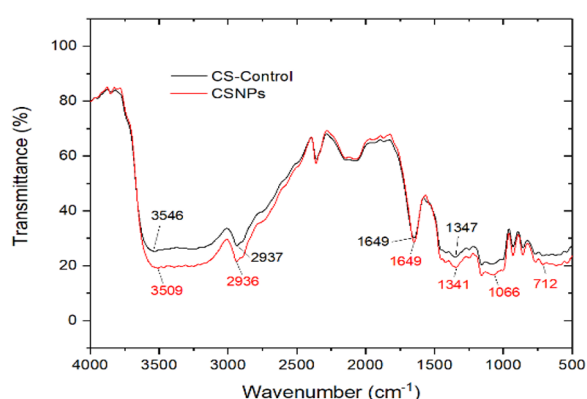


Fig. 2. FTIR of CSNPs and Native Starch

In the fingerprint region (1150–900  $\text{cm}^{-1}$ ), the CSNPs exhibited a sharper profile and subtle intensity shifts in the C–O–C and CH/CH<sub>2</sub> bending zones, indicating an enrichment of short-range order. Specifically, an increase in the A1047/A1022 (or A1047/A995) ratio reflects a higher density of double-helical structures, a phenomenon that correlates with reduced swelling and enhanced thermal resistance in modified starches [21]. Unlike treatments that induce distinct chemical modifications such as biomass surfactants on coal which present entirely new functional groups the acid treatment of starch is a process of refining existing structures [20]. Consequently, the FTIR data serves as a molecular explanation for the observed functional behavior: a more ordered, re-associated matrix that better resists water penetration and shear disruption.

### 3.3 Morphology (SEM/TEM)

SEM images of figure 3b the hydrolyzed material showed pervasive surface pitting, rounding of once-faceted granules, and the presence of fine debris around partially collapsed particles, in contrast to the textbook, well-defined granules of CS-Control. This is the morphological fingerprint of top-down acid hydrolysis of starch: acids enter through the more disordered lamellae, erode them, and leave behind more compact crystalline remnants [12]. The fact that bulk properties all decreased (solubility, swelling, moisture) is therefore fully

consistent with what it seen on the surface fewer open pathways for water and fewer long chains available to disentangle.

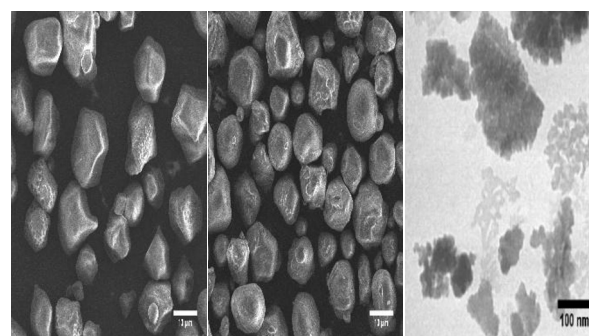


Fig. 3a. SEM CS-Control, 3b. SEM CSNPs, 3c. TEM CSNPs

Morphology and Aggregation Behavior as shown in Figure 3c, Transmission Electron Microscopy (TEM) reveals that the 2.2 N HCl treatment successfully produced primary particles ranging from tens to hundreds of nanometers. However, these nanoscale building blocks tend to cluster into soft aggregates or flocs. This morphological profile is consistent, where TEM confirms the generation of nanosized objects that remain prone to aggregation due to the inherent starch surface chemistry and weakly negative zeta potential [17], [22]. Because the acid treatment does not sufficiently alter the surface charge, these nanocrystals lack the electrostatic repulsion necessary to overcome the strong inter-particle hydrogen bonding, a phenomenon common in both potato and quinoa starch systems [15], [23]. Aggregation behavior directly explains the Dynamic Light Scattering (DLS) results, which showed a main intensity mode near 1 $\mu\text{m}$ . Intensity-weighted DLS is highly sensitive to larger particles and overemphasizes even a small population of clusters within the dispersion [22]. Consequently, while TEM provides visual proof of the nanosized primary particles, the DLS data reflects the actual state of the suspension nanoscale fragments that have re-associated into larger flocs [23]. This disparity highlights a significant challenge in starch nanotechnology: while hydrolysis effectively breaks down the starch matrix into building blocks, maintaining a stable, non-aggregated nanoscale suspension requires additional processing, such as ultrasonication or the introduction of steric stabilizers to disrupt these hydrogen-bonded clusters [15], [24].

### 3.4 Zeta potential ( $\zeta$ ), PDI(Polydispersity Index), and particle-size distribution

As shown in Figure 4, both samples exhibited weakly negative zeta potential values approximately -8.01mV for CS-Control and -7.73mV for CSNPs with a marginal narrowing of the Polydispersity Index (PDI) from 0.472 to 0.427. This indicates that while acid hydrolysis reorganizes the polysaccharide structure, it does not introduce new ionizable groups, resulting in minimal surface charge modification [23], [25]. Studies emphasize that even when hydrolysis improves wettability, zeta potential values typically remain above the -30mV

threshold required for electrostatic stability [26]. Consequently, the surface charge remains insufficient to provide long-term stabilization, causing particles to aggregate unless additional stabilization strategies are employed [3], [27].

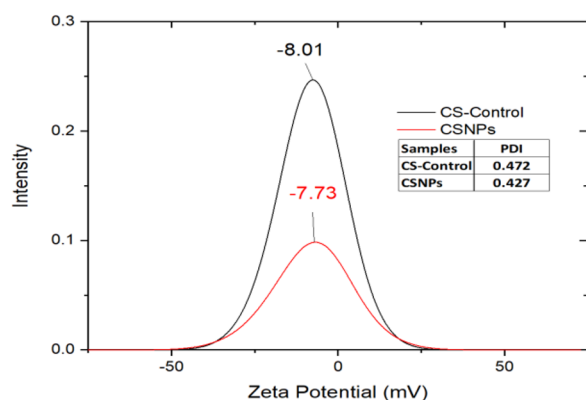


Fig. 4. Zeta potential & PDI

Data in Figure 5 further confirms this behavior. The Z-average diameter decreased from  $\approx 4.9 \mu\text{m}$  to  $3.8 \mu\text{m}$ , and the large-size shoulder of the native starch nearly disappeared, indicating that the acid treatment successfully reduced the largest aggregates. However, the main intensity mode remained near  $1 \mu\text{m}$  due to the clustering of nanoscale fragments in water [26], [27]. This trend highlights that while hydrolysis is effective at breaking down large clumps, it does not inherently produce a stable nanoparticle suspension. From a formulation perspective, achieving true nanoscale dispersion necessitates mandatory post-processing steps, such as pH/ionic strength adjustments to increase surface charge, ultrasonication, or the addition of steric stabilizers like maltodextrin or PVA [23], [27].

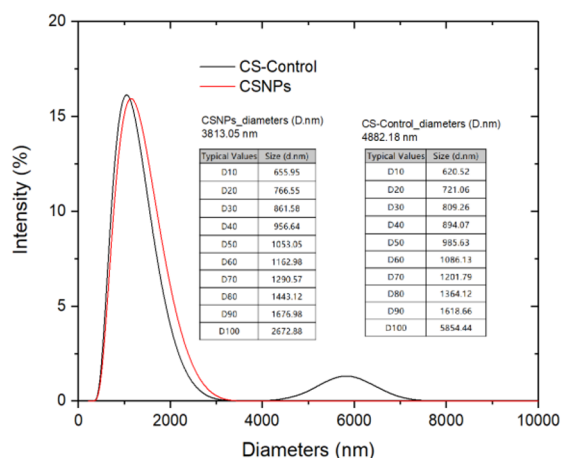


Fig. 5. Particle size

Acid hydrolysis of commercial corn starch with 2.2 N HCl at 35 °C for 120 h successfully transformed native starch (CS-Control) into a nano-enabled, more ordered material (CSNPs). The hydrolysed starch consistently showed lower apparent amylose (14.78  $\rightarrow$  13.61%), lower swelling (17.86  $\rightarrow$  16.58%), lower solubility (19.95 $\rightarrow$ 14.69%), lower moisture (10.95  $\rightarrow$  8.91%), and lower protein/fat than the control,

indicating that the acid primarily removed amorphous/less ordered regions and allowed the remaining chains to repack through stronger hydrogen bonding. FTIR supported this bands typical of starch were retained no new chemistry or bond created, but the O–H region became slightly more bonded and the 1150–900  $\text{cm}^{-1}$  fingerprint became sharper, signaling reduced amorphous content. SEM showed etched, rounded, debris-covered granules, and TEM confirmed the presence of tens-hundreds of nm fragments that aggregated, which explains why DLS still detected submicron/micron populations the process creates nanos but does not disperse them.

## 4 Conclusion.

Acid hydrolysis of commercial corn starch with 2.2 N HCl at 35 °C for 120 h successfully transformed native starch (CS-Control) into a nano-enabled, more ordered material (CSNPs). The hydrolyzed starch consistently showed lower apparent amylose (14.78  $\rightarrow$  13.61%), lower swelling (17.86  $\rightarrow$  16.58%), lower solubility (19.95 $\rightarrow$ 14.69%), lower moisture (10.95  $\rightarrow$  8.91%), and lower protein/fat than the control, indicating that the acid primarily removed amorphous/less ordered regions and allowed the remaining chains to repack through stronger hydrogen bonding. FTIR supported this bands typical of starch were retained no new chemistry or bond created, but the O–H region became slightly more bonded and the 1150–900  $\text{cm}^{-1}$  fingerprint became sharper, signaling reduced amorphous content. SEM showed etched, rounded, debris-covered granules, and TEM confirmed the presence of tens-hundreds of nm fragments that aggregated, which explains why DLS still detected submicron/micron populations the process creates nanos but does not disperse them. Therefore, while acid hydrolysis is an effective method for isolating starch nanocrystals, future applications requiring discrete nanoscale dispersion should incorporate stabilization strategies, such as the addition of steric stabilizers (e.g., surfactants or polymers) or ultrasonic post-treatment, to prevent aggregation and fully exploit the high surface area of the nanomaterials.

## References

1. H. Marta, Y. Cahyana, S. Bintang, G. P. Soeherman, and M. Djali, Physicochemical and pasting properties of corn starch as affected by hydrothermal modification by various methods, *Int. J. Food Prop.*, vol. **25**, no. 1, pp. 792–812, (2022), <https://doi.org/10.1080/10942912.2022.2064490>
2. C. Qiu, J. Yang, S. Ge, R. Chang, L. Xiong, and Q. Sun, Preparation and characterization of size-controlled starch nanoparticles based on short linear chains from debranched waxy corn starch, *Lwt*, vol. **74**, pp. 303–310, (2016), doi: <https://doi.org/10.1016/j.lwt.2016.07.062>
3. D. Bajer, Nano-starch for food applications obtained by hydrolysis and ultrasonication methods,

- Food Chem., vol. **402**, no. September (2022), p. 134489, Feb. 2023, doi: <https://doi.org/10.1016/j.foodchem.2022.134489>
4. Q. Lin et al., Fabrication of debranched starch nanoparticles via reverse emulsification for improvement of functional properties of corn starch films, *Food Hydrocoll.*, vol. **104**, no. June 2019, (2020), <https://doi.org/10.1016/j.foodhyd.2020.105760>
  5. A. A. Escobar-Puentes, A. García-Gurrola, S. Rincón, A. Zepeda, and F. Martínez-Bustos, Effect of amylose/amylopectin content and succinylation on properties of corn starch nanoparticles as encapsulants of anthocyanins, *Carbohydr. Polym.*, vol. **250**, no. May, (2020), doi: [10.1016/j.carbpol.2020.116972](https://doi.org/10.1016/j.carbpol.2020.116972)
  6. Z. Liu, Y. Zhao, J. Zheng, Z. Wang, X. Yan, and T. Zhang, Physicochemical and digestive properties of corn starch nanoparticles incorporated different polyphenols, *Int. J. Biol. Macromol.*, vol. **265**, no. April, (2024), doi: <https://doi.org/10.1016/j.ijbiomac.2024.130681>
  7. M. G. Fawzy, W. E. Hassan, A. A. Mostafa, and R. A. Sayed, Different approaches for the assessment of greenness of spectrophotometric methodologies utilized for resolving the spectral overlap of newly approved binary hypoglycemic pharmaceutical mixture, *Spectrochim. Acta - Part A Mol. Biomol. Spectrosc.*, vol. **272**, p. 120998, (2022), doi: [10.1016/j.saa.2022.120998](https://doi.org/10.1016/j.saa.2022.120998)
  8. K. N. Baruah, S. Singha, and R. V. S. Uppaluri, Preparation of Potato Starch Nanoparticles Using Acid Hydrolysis and Ultrasonic Post-treatment, *ACS Food Sci. Technol.*, vol. **3**, no. 4, pp. 626–634, (2023), doi: <https://doi.org/10.1021/acsfoodscitech.2c00369>
  9. M. E. A. Mohsin et al., Optimization and Characterization of Acetic Acid-Hydrolyzed Cassava Starch Nanoparticles for Enhanced Oil Recovery Applications, *Polymers (Basel)*, vol. **17**, no. 8, pp. 1–25, (2025), doi: <https://doi.org/10.3390/polym17081071>
  10. H. Marta, D. I. Rizki, E. Mardawati, M. Djali, M. Mohammad, and Y. Cahyana, Starch Nanoparticles: Preparation, Properties and Applications, *Polymers (Basel)*, vol. **15**, no. 5, pp. 19–25, (2023), doi: <https://doi.org/10.3390/polym15051167>
  11. Q. Zhang, Y. Zhou, W. Yue, W. Qin, H. Dong, and T. Vasanthan, Nanostructures of protein-polysaccharide complexes or conjugates for encapsulation of bioactive compounds, *Trends Food Sci. Technol.*, vol. **109**, no. May 2020, pp. 169–196, (2021), <https://doi.org/10.1016/j.tifs.2021.01.026>
  12. L. Zhou et al., Preparation and characterization of waxy maize starch nanoparticles via hydrochloric acid vapor hydrolysis combined with ultrasonication treatment, *Ultrason. Sonochem.*, vol. **80**, no. November, (2021), doi: <https://doi.org/10.1016/j.ultsonch.2021.105836>
  13. D. D. Ramdath, Z. Lu, P. L. Maharaj, J. Winberg, Y. Brummer, and A. Hawke, Proximate Analysis and Nutritional Evaluation of and Cluster Analyses, *Foods*, vol. **9**, no. 175, pp. 1–16, 2020, doi: <https://doi.org/10.3390/foods9020175>
  14. Y. Ren, T. Z. Yuan, C. M. Chigwedere, and Y. Ai, A current review of structure, functional properties, and industrial applications of pulse starches for value-added utilization, *Compr. Rev. Food Sci. Food Saf.*, vol. **20**, no. 3, pp. 3061–3092, (2021), doi: [10.1111/1541-4337.12735](https://doi.org/10.1111/1541-4337.12735)
  15. L. E. Velásquez-Castillo, M. A. Leite, C. Ditchfield, P. J. do A. Sobral, and I. C. F. Moraes, Quinoa starch nanocrystals production by acid hydrolysis: Kinetics and properties, *Int. J. Biol. Macromol.*, vol. **143**, pp. 93–101, (2020), doi: <https://doi.org/10.1016/j.ijbiomac.2019.12.011>
  16. L. P. Wrasiasi et al., Green extraction method and microencapsulation of tannins from young coconut husks-based food waste using gelatin/nanofiber cellulose, *Case Stud. Chem. Environ. Eng.*, vol. **11**, no. March, p. 101210, Jun. (2025), doi: <https://doi.org/10.1016/j.csee.2025.101210>
  17. C. Qiu et al., A review of green techniques for the synthesis of size-controlled starch-based nanoparticles and their applications as nanodelivery systems, *Trends Food Sci. Technol.*, vol. **92**, no. October (2018), pp. 138–151, 2019, doi: <https://doi.org/10.1016/j.tifs.2019.08.007>
  18. T. Hong, J. Y. Yin, S. P. Nie, and M. Y. Xie, Applications of infrared spectroscopy in polysaccharide structural analysis: Progress, challenge and perspective, *Food Chem. X*, vol. **12**, no. November, p. 100168, (2021), doi: <https://doi.org/10.1016/j.fochx.2021.100168>
  19. Y. Bi, H. Lei, Y. Fang, S. Wang, and J. Tang, Study on the Physical Properties and Application of a Novel Pharmaceutical Excipient Made from Starch and Cellulose Co-Processing, pp. 1–14, (2025). Doi: <https://doi.org/10.3390/ph18091389>
  20. L. Yang and Y. Yuan, Functional group characteristics of coal treated with clean biomass surfactant via FTIR spectroscopy, pp. 1–21, (2025). Doi: <https://doi.org/10.1038/s41598-025-03769-z>
  21. C. Pintilii et al., Food Chemistry : X Comparative study on starch and protein secondary structures in brown , red , and black rice influenced by microwave treatment, vol. **32**, no. October, 2025, doi: [10.1016/j.fochx.2025.102552](https://doi.org/10.1016/j.fochx.2025.102552)
  22. Y. Zhou, S. Sun, W. Bei, M. R. Zahi, Q. Yuan, and H. Liang, Preparation and antimicrobial activity of oregano essential oil Pickering emulsion stabilized by cellulose nanocrystals, *Int. J. Biol. Macromol.*, vol. **112**, pp. 7–13, (2018), doi: <https://doi.org/10.1016/j.ijbiomac.2018.01.102>
  23. B. Wei, X. Xu, Z. Jin, and Y. Tian, Surface Chemical Compositions and Dispersity of Starch

- Nanocrystals Formed by Sulfuric and Hydrochloric Acid Hydrolysis, vol. **9**, no. 2, pp. 1–7, (2014), doi: <https://doi.org/10.1371/journal.pone.0086024>
24. V. S. Hakke, U. D. Bagale, S. Bou, G. U. B. Babu, and S. H. Sonawane, Ultrasound Assisted Synthesis of Starch Nanocrystals and It ' s Applications with Polyurethane for Packaging Film, (2020), doi: <https://doi.org/10.32604/jrm.2020.08449>
  25. F. Fang, S. Cheng, and L. Huang, Structural modifications and physicochemical characterization of Pueraria lobata starch : Focusing on the impact of combined enzymatic and acid hydrolysis on emulsifying efficiency, vol. **495**, no. December, pp. 1–6, (2025). Doi : [10.1016/j.foodchem.2025.146647](https://doi.org/10.1016/j.foodchem.2025.146647)
  26. E. Mauret, A. Romdhane, and M. Aourousseau, Effect of pH and ionic strength on the electrical charge and particle size distribution of starch nanocrystal suspensions, pp. 319–327, (2015), doi: <https://doi.org/10.1002/star.201400181>
  27. E. Masoudipour, S. Kashanian, and A. Hemati, Surfactant effects on the particle size , zeta potential , and stability of starch nanoparticles and their use in a pH- responsive manner, Cellulose, (2017), doi: <https://doi.org/10.1007/s10570-017-1426-3>